Status Report: E05-103: Low Energy Deuteron Photodisintegration

Jackie Glister

Hall A Collaboration Meeting
June 14, 2008

Spokespeople: R. Gilman, A. Sarty & S. Strauch
Ph.D. Students: J. Glister & G. Ron
Undergraduate Students: J. Dumas, E. McCullough & Y. Rousseau

Deuteron Photodisintegration at Low Energies

- At lower photon energies, theoretical calculations based on meson-baryon degrees of freedom give a good description of cross-section and polarization observables
- Currently, the best model comes from Schwamb and Arenhövel (complete calculation is solid line in figures), where modern NN potentials and relativistic corrections have been incorporated

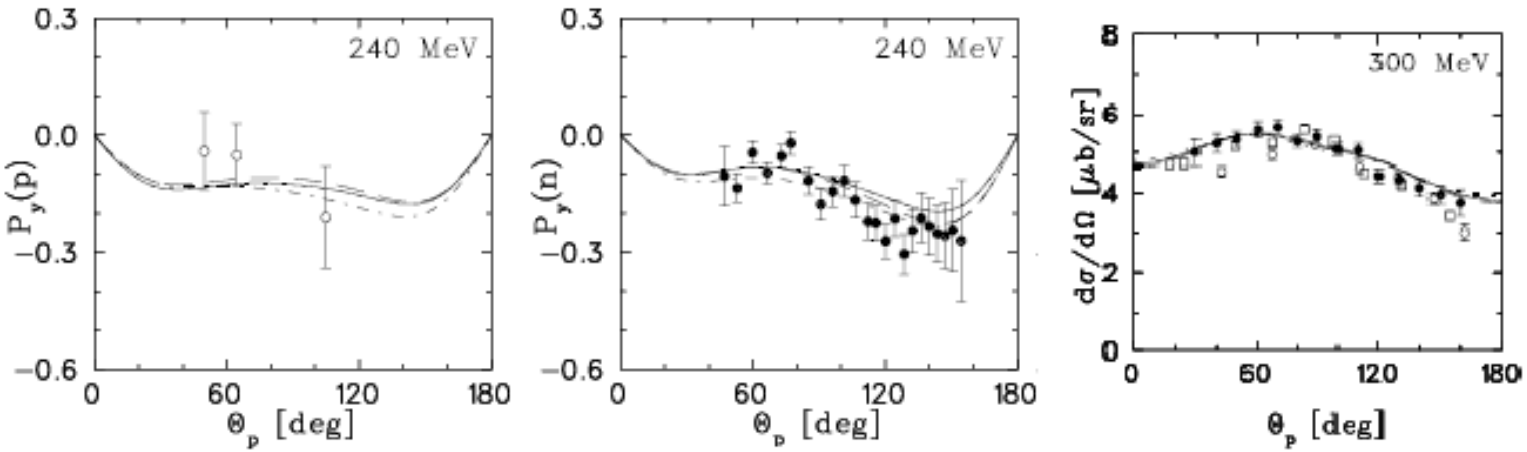

Figure: Nucl. Phys. **A690**, 682 (2001)

Observables

- $P^c_{x'} \Rightarrow$ transferred polarization in reaction plane, $\perp$ to $\vec{p}$
  Real part of sum of amplitudes
- $P_y \Rightarrow$ induced polarization, $\perp$ to reaction plane
  Imaginary part of same sum of amplitudes
- $P^c_{z'} \Rightarrow$ transferred polarization in reaction plane, $\parallel$ to $\vec{p}$
  Difference of amplitudes squared

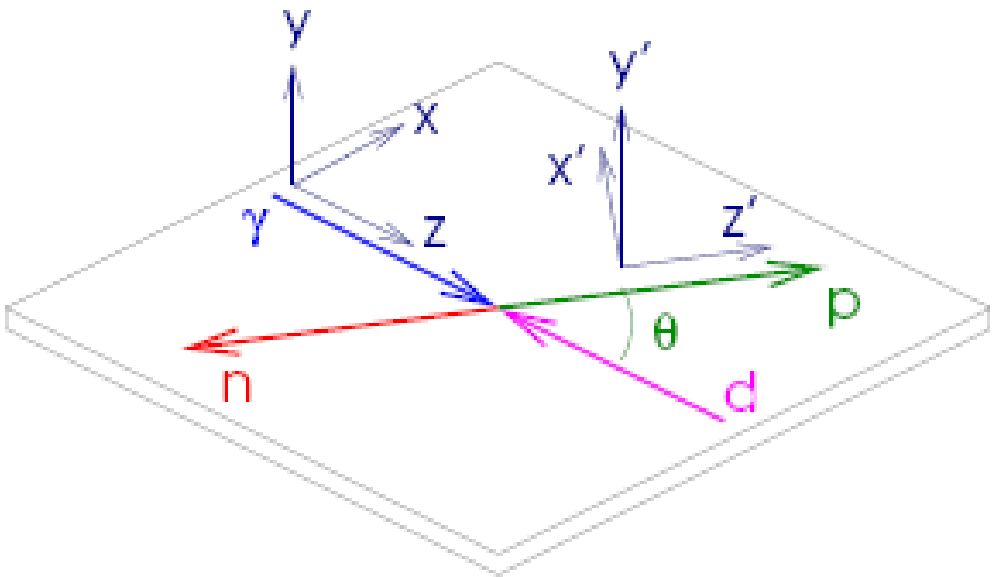

Discrepancy in Proton Polarization Observables

- As incident photon energy grows, a disagreement between world data and the calculation for P_y emerges around $\theta_{cm} = 90^o$
- No data for $P_x^{c'}$ and $P_z^{c'}$ in this energy region
- Motivation of experiment was to provide high-precision polarization data in the 300-400 MeV region to help resolve whether the problem lies with the data or the calculation

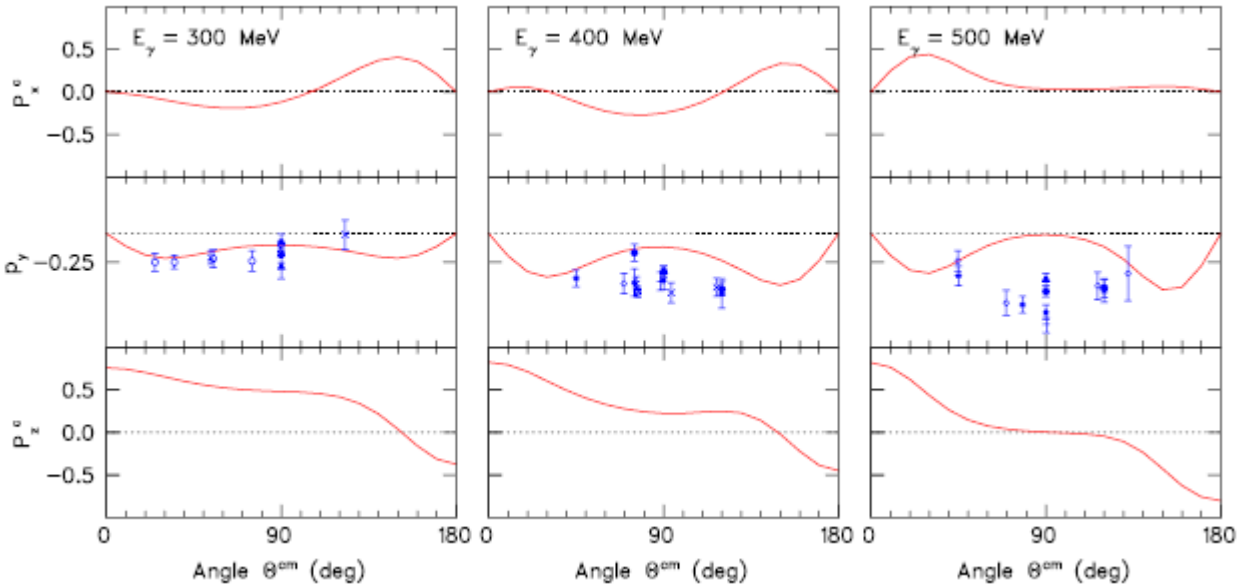

Deuteron Photodisintegration Reaction

- E_o = 361.7 MeV, giving photon energy endpoint of 361.2 MeV
- Bremsstrahlung photon production using copper radiator with 4% and 5% of a radiation length thickness
- Circularly polarized photon incident on 15 cm LD2
- Singles measurement with proton momentum kept above pion production threshold
- FPP carbon analyzer thickness increased with proton momentum: S2 + (0.75”, 2.25” and 3.75”)
- Polarization of 38 - 41%, except for last setting ($\theta_{cm} = 120^o$) when the Wien angle was changed and polarization was 72%

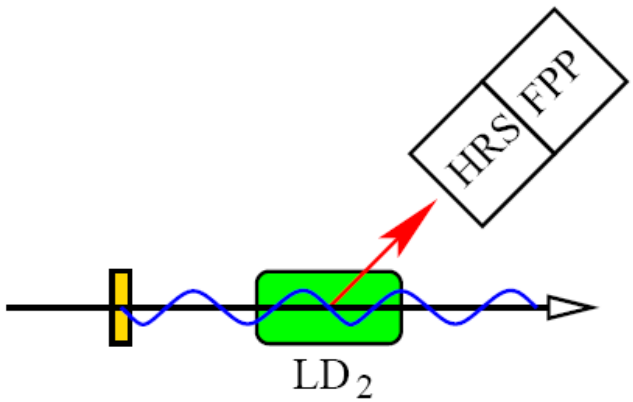

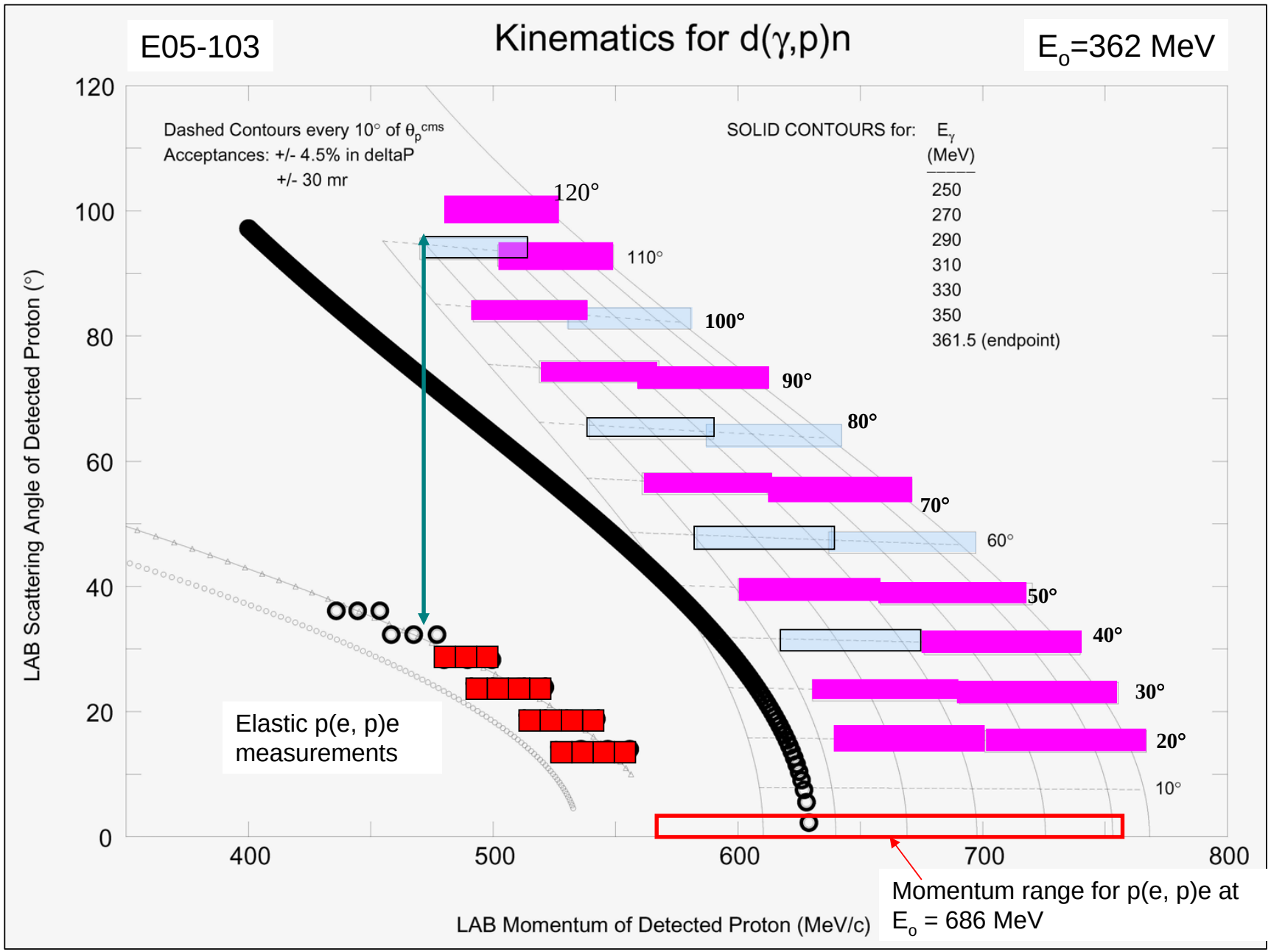
E05-103
Kinematics for d(γ,p)n
E0=362 MeV
Dashed Contours every 10° of θp cms
Acceptances: +/- 4.5% in deltaP
+/- 30 mr
SOLID CONTOURS for: Eγ (MeV)
250
270
290
310
330
350
361.5 (endpoint)
120°
110°
100°
90°
80°
70°
60°
50°
40°
30°
20°
10°
Elastic p(e, p)e measurements
Momentum range for p(e, p)e at E0 = 686 MeV
LAB Scattering Angle of Detected Proton (°)
LAB Momentum of Detected Proton (MeV/c)
0
20
40
60
80
100
120
400
500
600
700
800

Extracting Polarization Observables

The spin-orbit interaction between the proton and carbon analyzer nucleus results in an asymmetry in the azimuthal scattering angle, ϕ_{fpp}. Left-right asymmetry gives the vertical component, P_x^{fpp}, while the up-down asymmetry gives the horizontal component, P_y^{fpp}.

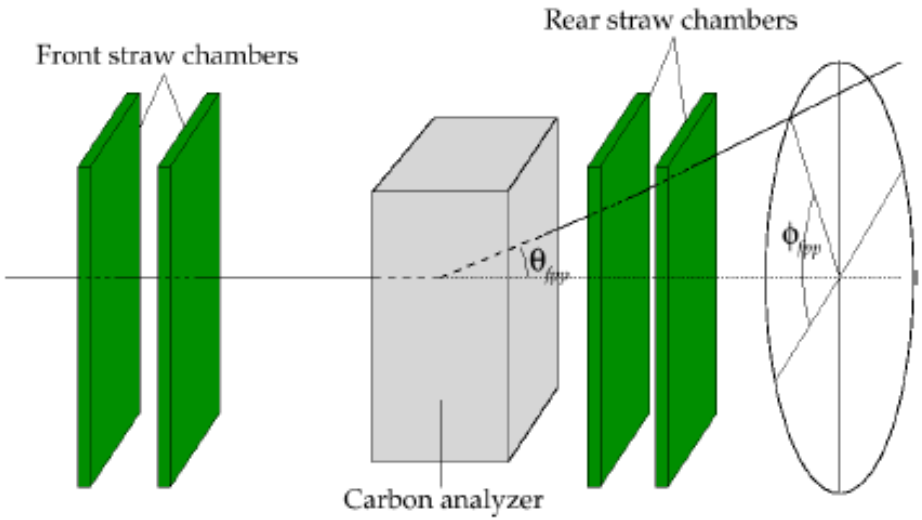

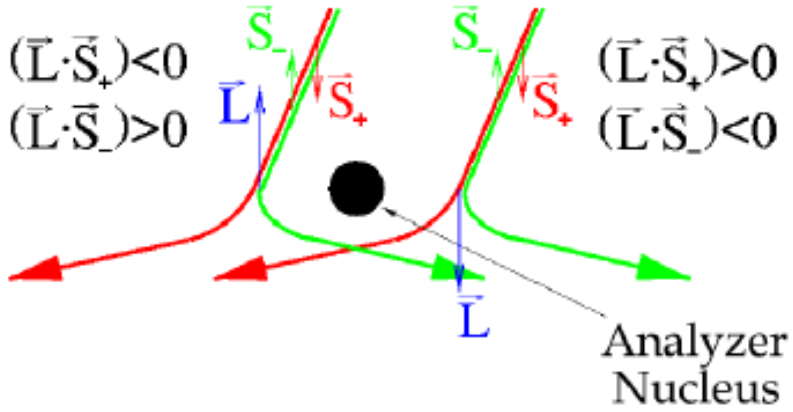

False Asymmetries

- False asymmetries, which do not cancel for induced polarizations as they do for transferred, are caused by FPP misalignments and inhomogeneities in detector efficiency
- Used cut on polar scattering angle of scatter ($\theta_{fpp} < 30^o$) to minimize false asymmetries at large angles
- FA be expanded as fourier series:

$$\xi = 1 + a \times cos(\phi_{fpp}) + b \times sin(\phi_{fpp}) + c \times cos(2\phi_{fpp}) + d \times cos(2\phi_{fpp}) \quad (1)$$

Parameterizing False Asymmetries

- In the single photon exchange approximation, induced polarization for elastic scattering is zero, allowing for direct measurement of instrumental asymmetries
- Excellent focal plane coverage of elastic data relative to production data, shown below left
- Parameterized fourier series coefficients as a function of δ_p, shown below right

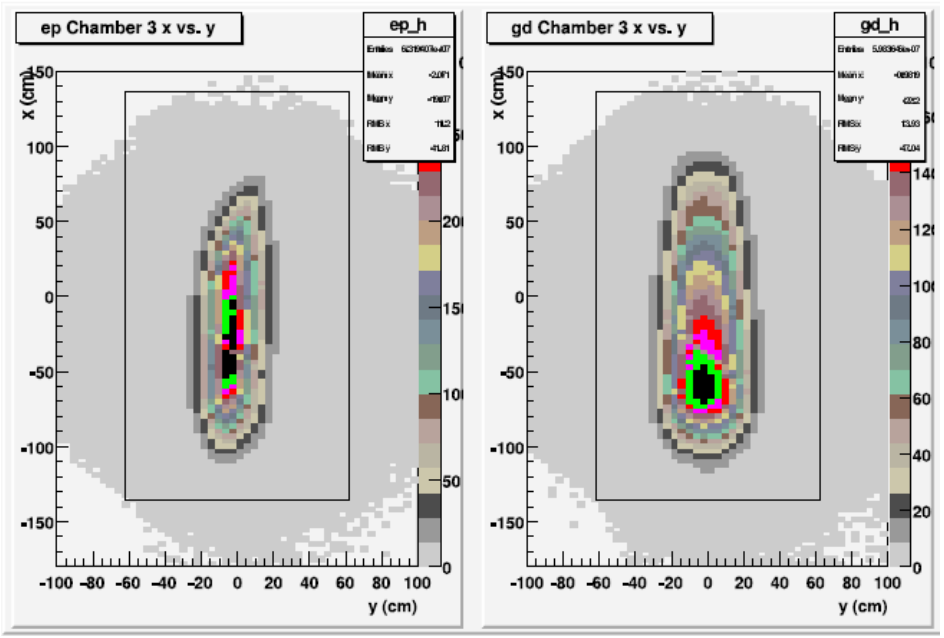

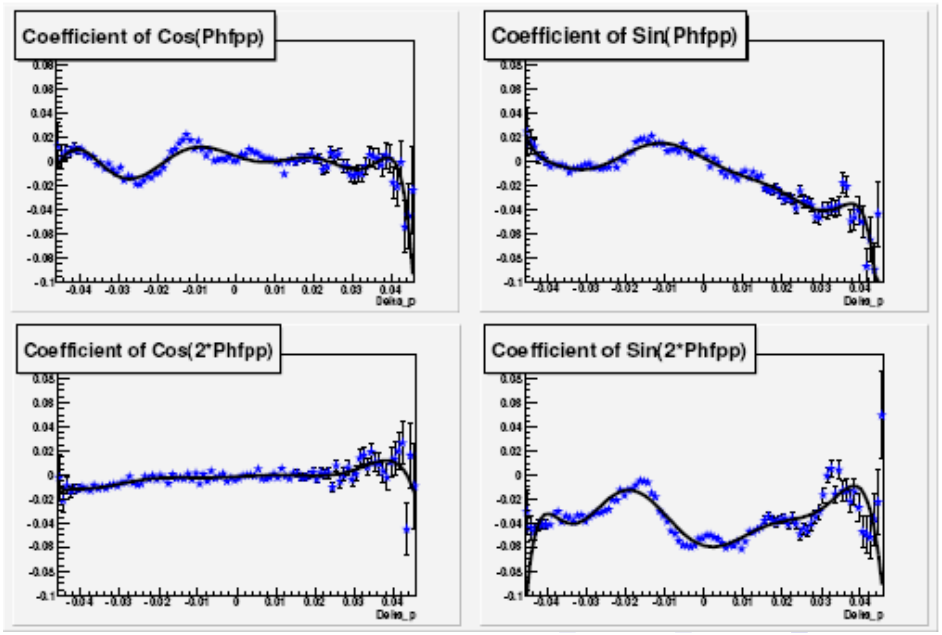

Result of Parameterization

Results of parameterization shown below as a function of ϕ_{fpp}. Top plot is helicity sum of elastic data for $0.015 < \delta_p < 0.025$, along with the instrumental asymmetry parameterization plotted for dp = 0.02. Bottom plot shows helicity sum subtracted by polynomial fit, resulting a flat distribution centered at zero.

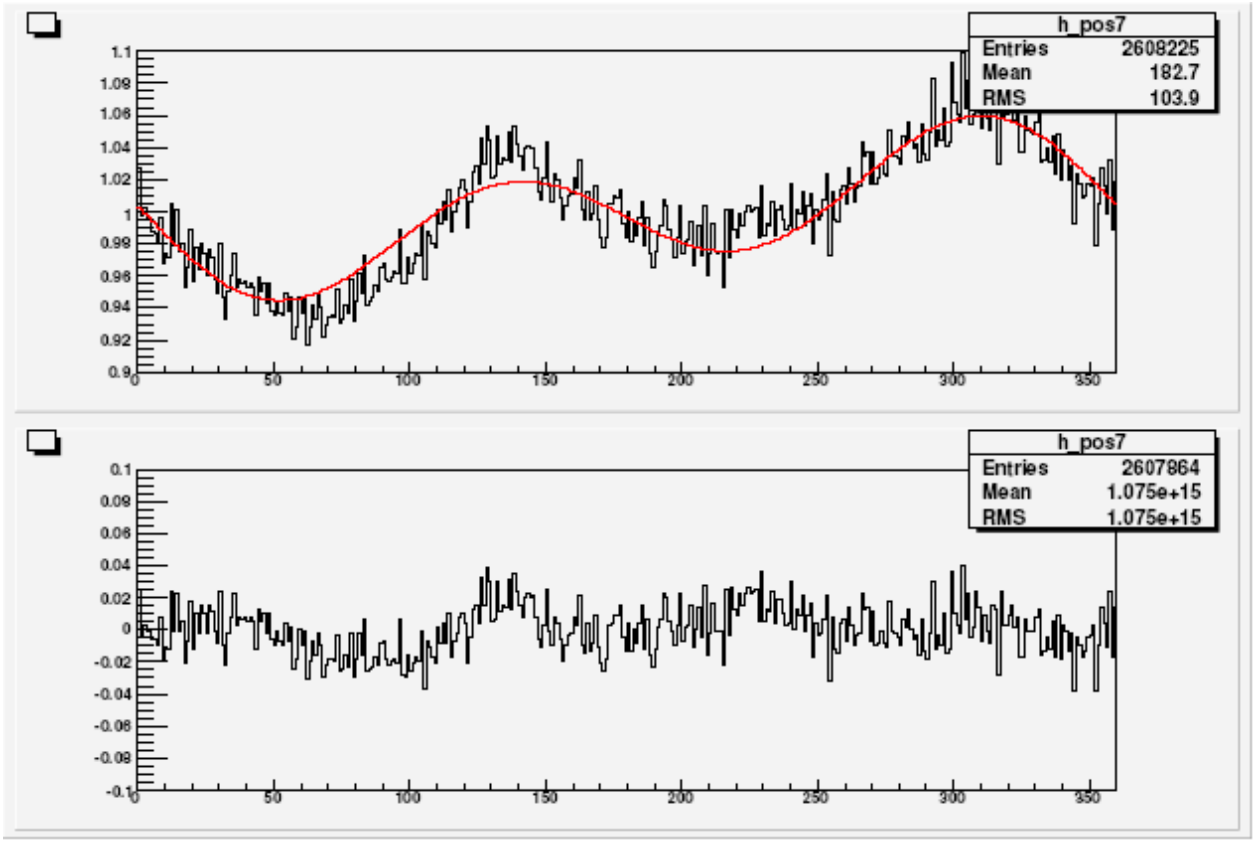

Spin Transport

- Three methods available to transport the spin through the spectrometer: simple dipole, Pentchev approximation and full COSY rotation
- The three methods give consistent results for all kinematic settings, except for the induced polarization at θ_{cm} = 70^o, 90^o and E = 360 MeV
- Cause is yet to be determined, one possibility is a large variation of COSY rotation matrix elements within those angular (70^o, 90^o $\pm$ 10^o, 360 $\pm$ 10 MeV)

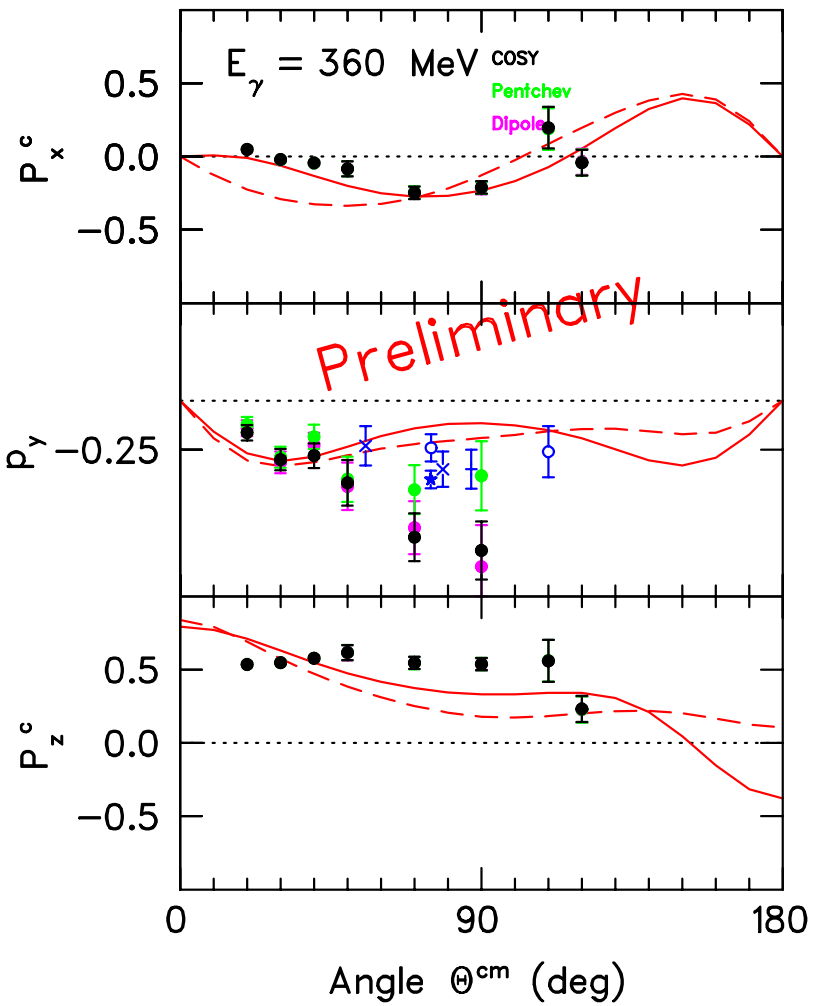

Systematics

- Uncertainties associated with spin rotation were calculated when the FPP was in the right arm and for a higher momentum range, they were conservatively doubled
- Systematics of target mispointing negligeable
- Errors associated with Analyzing Power and false asymmetry parameterizations were also considered

Variable	Shift
θ_{fpp}	2 mrad
ϕ_{fpp}	2 mrad
θ_{fp}-θ_{tg}	2×7 mrad
ϕ_{fp}-ϕ_{tg}	2×0.3 mrad
$(\phi_d \vert y_{tg})$	2×0.038
$(\phi_d \vert \phi_{tg})$	2×0.082
$(\Delta\phi_d \vert y_{tg})$	2×0.105
$(\Delta\phi_d \vert \phi_{tg})$	2×0.111
Mott stat	1.19 - 1.77% (abs)
Mott sys	1.82 - 2.04)% (abs)
Energy	2 MeV
Momentum	Rel. 10^{-3}

Results - Angular Dependence

- World data for P_y shown in blue; systematic uncertainties shown as black strips; Pentchev spin transport used
- Curves are Schwamb and Arenhövel, dashed are more recent (interactions in propagating πNN-system treated non-perturbatively, as opposed to only approximately)

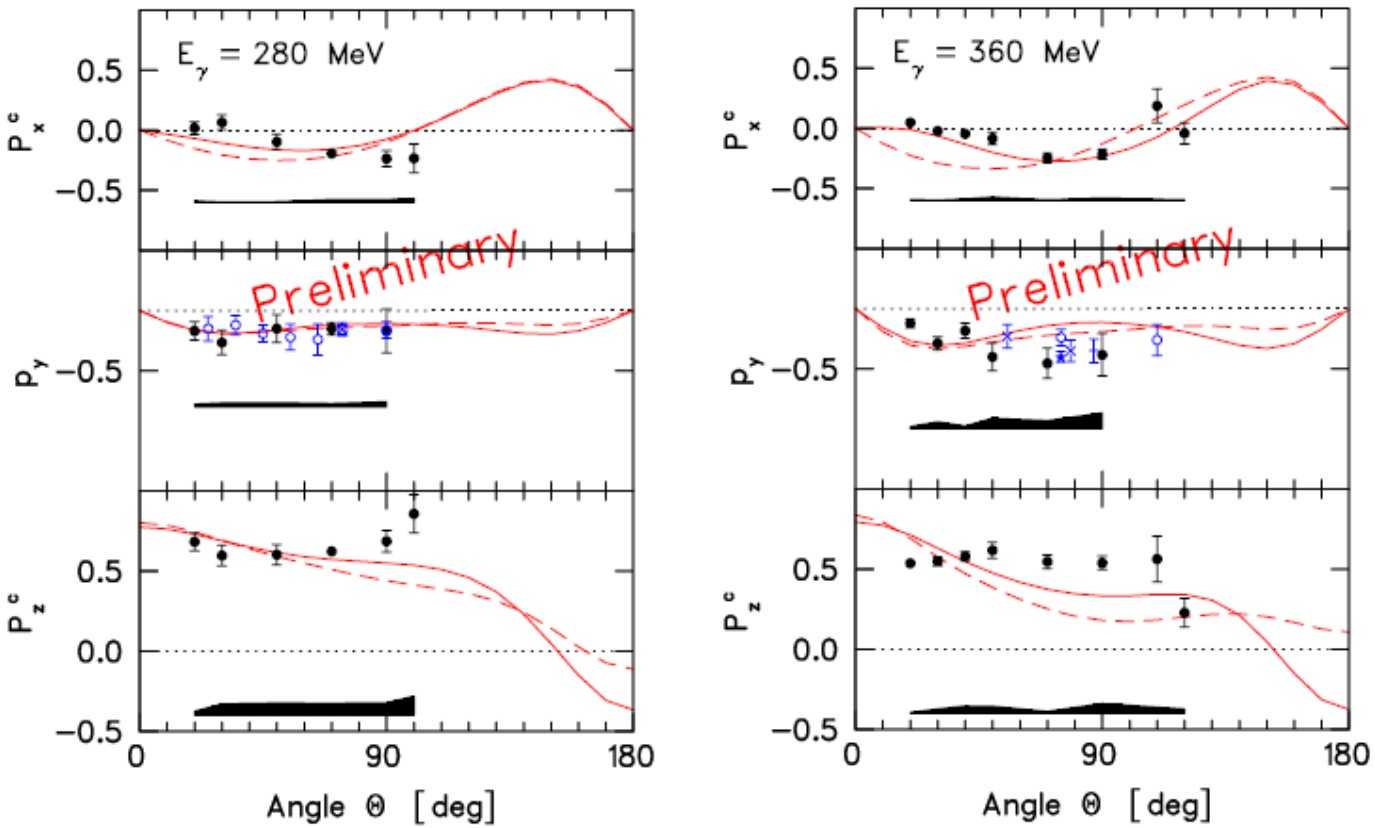

Summary

- Both P_x^c and P_z^c are in excellent agreement with the calculations of Schwamb and Arenhövel at the lowest energy
- As energy grows, it becomes clear that P_x^c has better agreement with the older calculation (solid line), while P_z^c appears to have a different shape from both curves
- Induced polarization appears to agree with the world data, indicating that something is missing in the current theoretical model